# Electronic Supporting Information

# Mixed-linker Approach in Designing Porous Zirconium Based Metal-Organic Frameworks with High Hydrogen Storage Capacity

Ayesha Naeem,[a] Valeska P. Ting,[b] Ulrich Hintermair,[b] Mi Tian,[b] Richard Telford,[a] Saaiba Halim,[a] Harriott Nowell,[c] Małgorzata Hołyńska,[d] Simon J. Teat,[e] Ian J. Scowen[f] and Sanjit Nayak[a*]

[a.] *School of Chemistry and Forensic Sciences, University of Bradford, Richmond Road, Bradford, West Yorkshire, BD7 1DP, United Kingdom*
[b.] *Department of Chemical Engineering, University of Bath, Claverton Down, Bath, BA2 7AY, UK*
[c.] *Diamond Light Source, Didcot, Oxon, OX11 0DE, UK*
[d.] *Fachbereich Chemie and Wissenschaftliches Zentrum für Materialwissenschaften, Philipps Universität Marburg, Hans-Meerwein-Straße, 35043 Marburg, Germany*
[e.] *Advance Light Source, Lawrence Berkeley National Laboratory, Berkeley, CA 94720 USA*
[f.] *School of Chemistry, University of Lincoln, Brayford Pool, Lincoln, Lincolnshire, LN6 7TS, United Kingdom*
**Corresponding author: s.nayak@bradford.ac.uk*

## List of content:

## 7. Thermogravimetric analyses



## 8. Gas sorption studies

# 1. Methods

## 1.1. Physical measurements:

Elemental analyses (CHN) were carried out on a Perkin-Elmer 2400 series II analyzer. Infrared spectra were recorded using reflectance technique over the range of 4000-500 $cm^{-1}$ on a Perkin-Elmer Spectrum 100 FTIR spectrometer fitted with a Perkin-Elmer Universal ATR sampling device. Thermogravimetric analyses were performed on a TA Q5000IR Thermogravimetric Analyzer (TA Instruments), under a 25 mL/min air purge gas flow and a 5 °C/min heating ramp. Scanning electron microscope (SEM) images were collected using E-SEM FEI Quanta 400 instrument. $^1H$ NMR data were collected on a Jeol ECA 600 spectrometer operating at 600.17 MHz for $^1H$. Spectra were acquired with 256 scans using a solvent suppression method (presaturation) to reduce the intensity of the HOD resonance.

PXRD measurements were obtained using a Bruker D8 Discover equipped with a rotating capillary stage, focussing Göbel-mirror, and a PSD Lynxeye® in θ-2θ geometry. Cu $K\alpha_{1,2}$-radiation (λ= 0.154018 nm, 1600W) was used in for the measurement. Samples were prepared in 0.7mm capillary and data was obtained in the range of 2θ = 2.5°- 50° with a scan step of 0.02° and 5s per step.

**Crystallography:**

X-ray Structure Determinations of **UBMOF-8 and UBMOF-9**: Crystals were mounted in the 250(2) K nitrogen cold stream provided by an Oxford Cryosystems Cryostream 800 Plus low-temperature apparatus on the goniometer head of a Bruker D8 diffractometer equipped with a PHOTON100 CMOS detector on beamline 11.3.1 at the Advanced Light Source in Berkeley, CA. Diffraction data were collected using synchrotron radiation, monochromated using silicon(111) to a wavelength of 0.77490(1) Å. An approximate full sphere of data was collected shutterless with 1° ω-scans. The data were integrated using the program SAINT V8.34A. A multi-scan correction for absorption was applied using the program SADABS-2014/5. Unit cell measurement of UBMOF-31 was performed using intensity data collected on a Bruker APEX II X8 diffractometer using Mo ($K_\alpha$) radiation at 173 K.

## 1.2. Gas sorption and surface area measurements:

**Experimental detail for high pressure hydrogen sorption studies:**

- High pressure gas sorption isotherms were collected on a Hiden Isochema HTP-1 volumetric gas sorption analyser, using an immersion dewar for temperature control at 77 K.
- Skeletal densities were determined using *in-situ* Helium pycnometry at room temperature
- Samples were degassed in a vacuum oven at ($10^{-3}$ mbar) at 150 °C for 8 hours prior to analysis.
- Uptake was calculated on a dry weight basis of degassed sample

wt% uptake = (wt $H_2$)/(wt sample)

**Experimental detail for comparison of $H_2$ adsorption at 77 K:**

- Liquid nitrogen immersion dewar used for temperature control at 77 K.
- Isotherms were run using Air Products BIP-Plus hydrogen (99.99996%) up to a max pressure of 120 bar (12 MPa)
- Skeletal densities were determined using *in-situ* He pycnometry at room temperature
- Samples were degassed for 2 hours *in-situ* at 150 °C under dynamic high vacuum ($10^{-6}$ mbar) between each sorption run.
- Repeated adsorption-desorption runs were collected to check for consistency of results. UBMOF-9 showed complete reversibility, typical of Type 1 sorption.

**Experimental detail for $CO_2$ and $N_2$ sorption at 0 °C:**

- An ice slurry used for temperature control at 273 K.
- Isotherms were run using BOC standard grade $N_2$ and $CO_2$ up to a maximum pressure of 25 bar (2.5 MPa) to avoid reverse sublimation of $CO_2$.
- Samples were degassed for 2 hours *in-situ* at 150 °C under dynamic high vacuum ($10^{-6}$ mbar) between each sorption run.
- Repeated measurements showed good repeatability and reversibility of both $CO_2$ and $N_2$ uptake, indicating pure physisorption.

## 2. General synthesis

All the chemicals were purchased from Sigma Aldrich, and used as received. The solvents were purchased from Fischer Scientific.

**2.1. UBMOF-8:** In a rubber lined glass vial 0.035 g of $ZrCl_4$ (0.15 mmol) and 0.50 g (4 mmol) of benzoic acid was dissolved in 2.5 mL dimethylformamide and 0.5 mL N-Methyl-2-pyrrolidone (NMP). The mixture was then sonicated at 50 °C for 20 min. To this solution 0.036 g (0.12 mmol) of $NH_2SDCAH_2$ was added and sonicated further for 30 minutes. The resulting solution was then placed into an oven programmed to heat at a ramp of 10 °C per minute to 120 °C. The temperature was maintained for 96 hours followed by cooling to 20 °C at a rate of 0.2 °C per minute. Reddish-brown octahedral crystals were obtained with yellow powder at the bottom of the vial.

Chemical Formula (vacuum dried sample): $[Zr_6O_4(OH)_4(DASDCA)_6]$; $C_{96}H_{92}N_{12}O_{32}Zr_6$; Elemental Analysis: (calcd.) C, 46.93; H, 3.12; N, 6.84; found: C, 48.84; H, 4.41; N, 5.43

**2.2. UBMOF-9:** In a rubber lined glass vial 0.101 g of $ZrCl_4$ (0.43 mmol) and 1.03 (8.4 mmol) g of benzoic acid was dissolved in 7 mL dimethylformamide and 1.5 mL N-Methyl-2-pyrrolidone (NMP). The mixture was then sonicated at 50 °C for 20 min. To this solution 0.101 g (0.38 mmol) of $SDCAH_2$ was added and sonicated further for 30 minutes. The resulting solution was then placed into an oven programmed to heat at a ramp of 10 °C per minute to 120 °C. The temperature was maintained for 96 hours followed by cooling to 20 °C at a rate of 0.2 °C per minute. Pale white crystals were obtained on the wall and at the bottom of the vial (Yield: 0.119 g)

Chemical Formula (vacuum dried sample): $[Zr_6O_4(OH)_4(SDCA)_6](PhCOOH)_{0.75}$; $C_{101.25}H_{68.5}O_{33.5}Zr_6$ (MW: 2368.47); Elemental Analysis (%): (calcd.) C, 51.35; H, 2.92; N, 0.00; % found: C, 50.77; H, 2.66; N, 0.05

**2.3. UBMOF-31:** In a rubber lined glass vial 0.101 g of $ZrCl_4$ (0.43 mmol) and 1.03 g of benzoic acid was dissolved in 7 mL dimethylformamide and 1.5 mL N-Methyl-2-pyrrolidone (NMP). The mixture was then sonicated at 50 °C for 20 min. To this solution 0.067 g (0.25 mmol) of $SDCAH_2$ and 0.030 g (0.1 mmol) of $NH_2SDCAH_2$ was added and sonicated further for 30 minutes. The resulting solution was then placed into an oven programmed to heat at a ramp of 10 °C per minute to 120 °C. The temperature was maintained for 96 hours followed by cooling to 20 °C at a rate of 0.2 °C per minute. Golden yellow crystals were obtained on the wall and at the bottom of the vial (Yield: 0.114 g)

Chemical Formula (vacuum dried sample): $[Zr_6O_4(OH)_4(DASDCA)_{1.4}(SDCA)_{4.6}](PhCOOH)_{0.78}$; $C_{101.46}H_{71.48}N_{2.8}O_{33.56}Zr_6$ (MW: 2414.18); Elemental Analysis: (calcd.) C, 50.48; H, 2.98; N, 1.62; found: C, 49.90; H, 3.14; N, 1.54

**2.4. Stability tests in different solvents:**

In a 12 mL rubber lined glass vial 50 mg of MOF sample was weighed followed by addition of 5 mL of corresponding solvent (distilled water or acetone). One set of the sample was left at room temperature (20 °C) for 24 hours, and the other set was placed in an oven which was heated to 100 °C at a ramp of 10 °C/min, and held at 100 °C for 24 hours followed by cooling to 20 °C at a ramp of 10 °C/min. The samples were then filtered and dried under air before powder X-ray diffraction and other characterizations.

# 3. Single-crystal X-ray diffraction

## 3.1. Details of the refinements

Both structures were solved by direct methods in SHELXS97 and refined in SHELXL97 [S1].
Both compounds are isostructural, crystallizing in the centrosymmetric space group type $Fm\bar{3}m$. Attempts to lower the space group symmetry resulted in analogous symptoms of disorder, therefore the highest-symmetry variant was retained.
The asymmetric unit contains one Zr1 atom (*48i* position, 4m.m site symmetry), one Zr-bridging O3 atom (*32f*, site symmetry .3m) and half of the stilbene ligand in both cases. The ethene fragment is disordered in two positions related by a symmetry plane which is a symmetry-induced disorder. In case of UBMOF-8 the location of the ligand required also a symmetry-induced disorder of the phenyl-bound amino group which adopts two positions on the two sides of the phenyl ring, related by a mirror symmetry plane. Charge balance requires the presence of one dinegative anion, two hydroxide ligands and 0.667 water ligands per one $Zr^{4+}$ cation.
DFIX restraints were used for the ethene C6=C6' bond, the C5-C6 bond joining the ethene and phenyl moiety along with the C6(ethene)…C4(phenyl) distance to regulate the C6-C5-C4 bond angle. For UBMOF-8 additionally the 1,4-distances in the ligand's phenyl ring were fixed. EADP restraints were used for all C atoms of the phenyl ring and ethene moiety, in UBMOF-8 including also the amine N1 atom. The presence of large voids filled with spurious disordered solvent (see the article text) required the use of SQUEEZE within the PLATON procedures [S2]. As mixed solvents were used, it is impossible to assess the solvent content in a reliable manner based on X-ray diffraction data only. The formulae in Table S3.1 correspond to the formulae excluding any solvent and modulator present in the compounds.
The highest difference Fourier peaks (0.78/0.82 e/Å$^3$ for UBMOF-9 and UBMOF-8, respectively) could not be assigned any reasonable interpretation and should be regarded as artefacts caused by the limited data quality and the use of SQUEEZE.

**Table S3.1.** Selected X-ray data for UBMOF-9 and UBMOF-8.

| | **UBMOF-9** | **UBMOF-8** | **UBMOF-31** |
|---|---|---|---|
| Formula | $C_{96}H_{80}O_{32}Zr_6$ | $C_{96}H_{92}N_{12}O_{32}Zr_6$ | Unit cell measurement |
| CCDC ref. number | 1440759 | 1440758 | |
| Formula weight | 2292.92 | 2473.14 | |
| Temperature [K] | 250(2) | 250(2) | 173(2) |
| λ [Å] | 0.77490 | 0.77490 | 1.54184 |
| Crystal system | Cubic | Cubic | Cubic |
| Space group | $Fm\bar{3}m$ | $Fm\bar{3}m$ | $Fm\bar{3}m$ |
| a [Å] | 29.941(1) | 29.983(2) | 29.317(7) |
| V [$Å^3$] | 26841(2) | 26954(3) | 25198(6) |
| Z, $\rho_{calc}$ [g $cm^{-3}$] | 4, 0.567 | 4, 0.609 | |
| μ [$mm^{-1}$] | 0.32 | 0.32 | |
| F(000) | 4608 | 4992 | |
| Crystal size [mm] | 0.1x0.1x0.06 | 0.120x0.080x0.080 | 0.1x0.1x0.05 |
| θ range[°] | 2.10-31.65 | 2.09-30.52 | |
| rflns: total/unique | 79732/1785 | 74251/1631 | |
| R(int) | 0.0442 | 0.0451 | |
| Abs. corr.<br>Min., max. transmission factors | multi-scan<br>0.624, 0.746 | multi-scan<br>0.684, 0.746 | |
| Data/restraints/params | 1785/6/30 | 1631/11/33 | |
| GOF on $F^2$ | 1.021 | 1.034 | |
| R1 [$I > 2\sigma(I)$] | 0.0549 | 0.0559 | |
| $wR_2$ (all data) | 0.1635 | 0.1820 | |
| Max., min. $\Delta\rho_{elect}$ [e $Å^{-3}$] | 0.78, -0.79 | 0.82, -0.69 | |

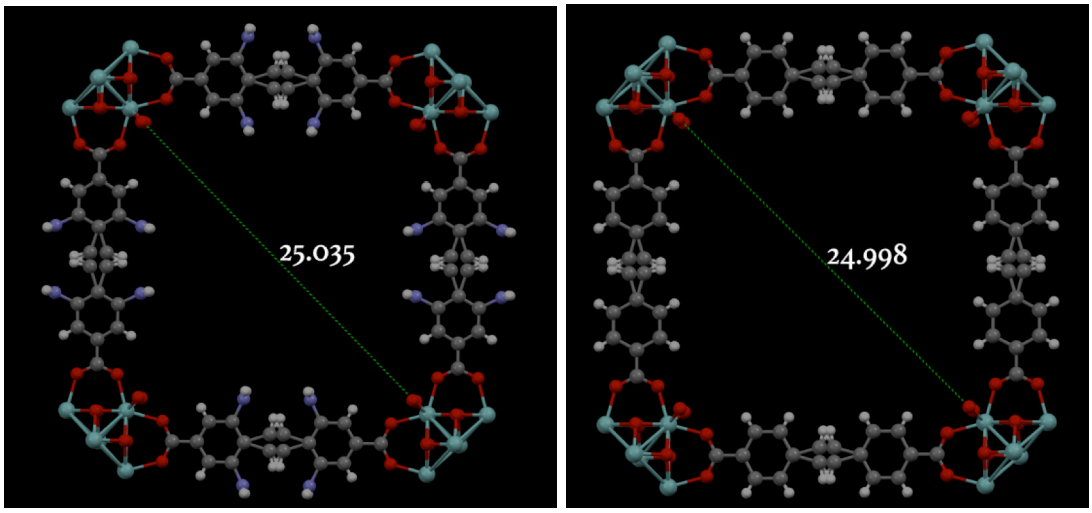


(A) (B)

**Figure S3.1.** Diagonal dimensions of the cages inside (A) UBMOF-8 and (B) UBMOF-9 are shown.

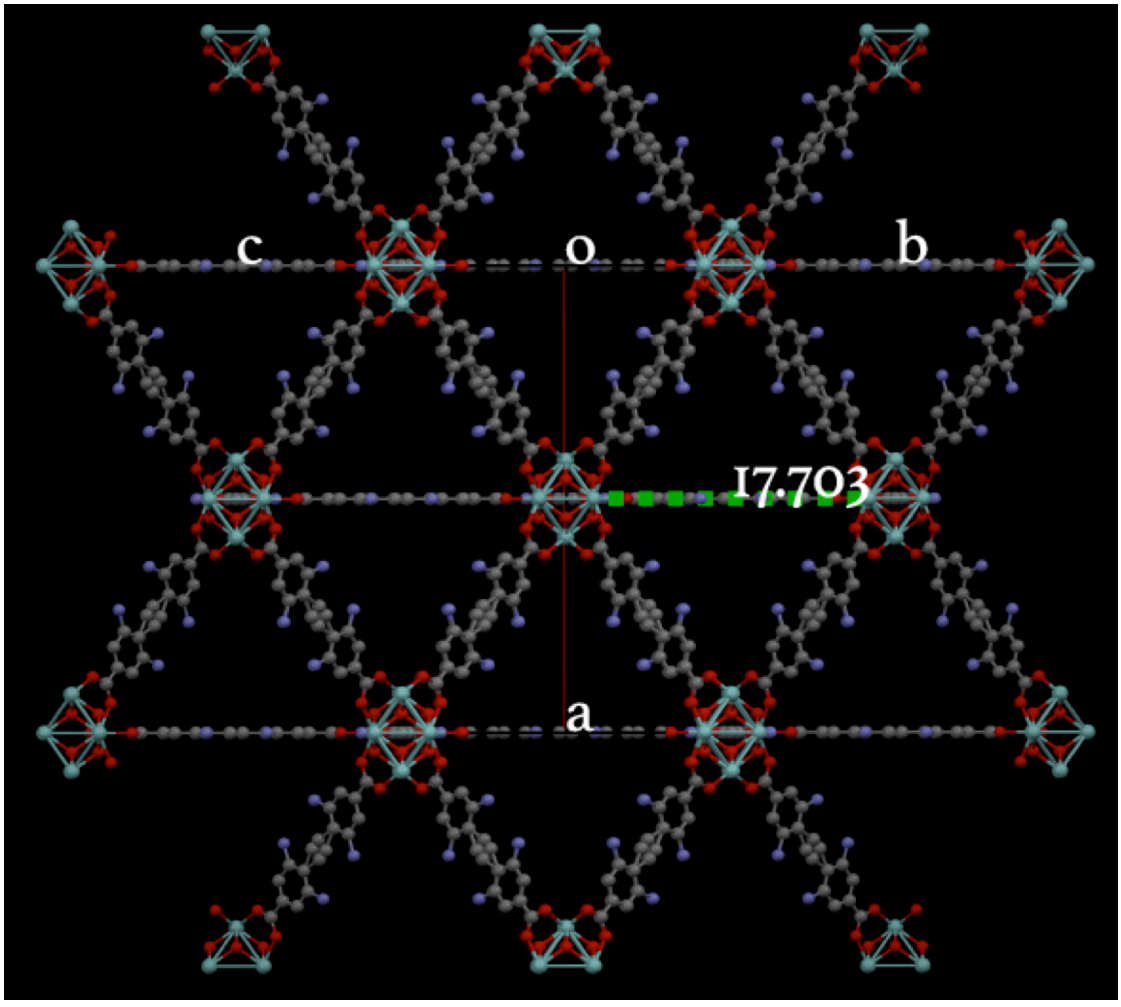


**Figure S3.2.** Dimension of the triangular faces of UBMOF-8 is shown.

# 4. Infrared spectra

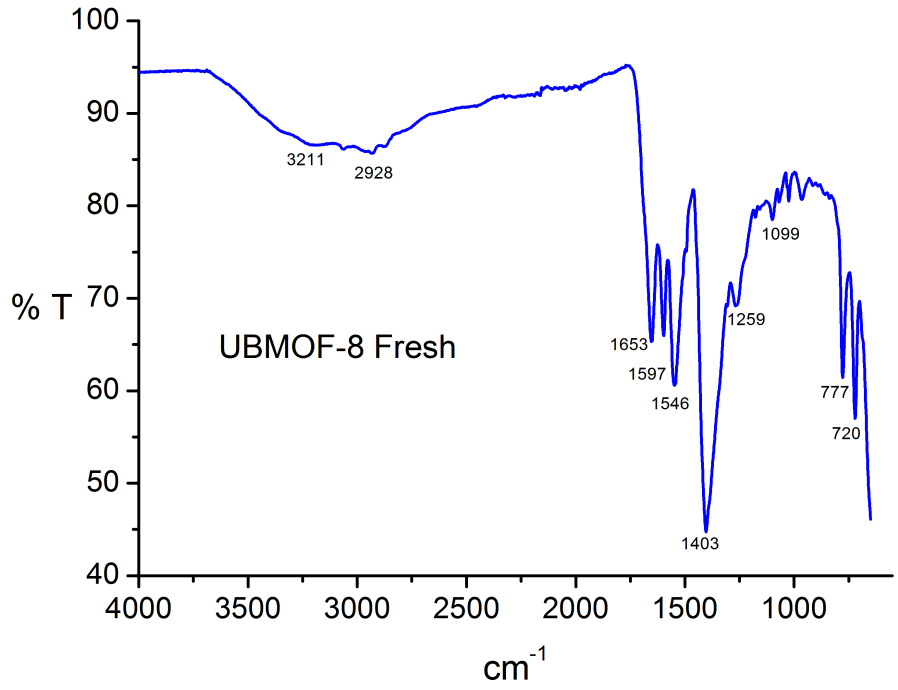


**Figure S4.1.** Infrared spectra of pristine UBMOF-8

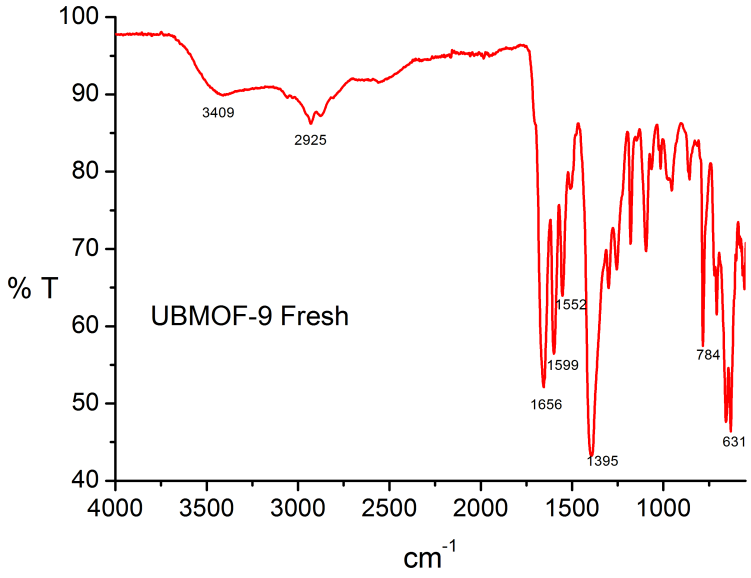


**Figure S4.2.** Infrared spectra of pristine UBMOF-9

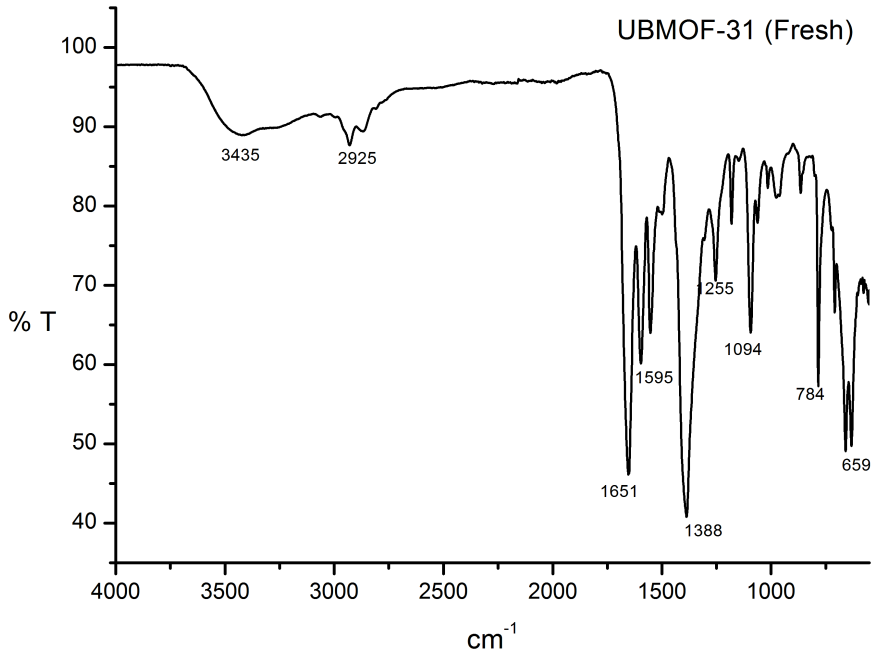


**Figure S4.3.** Infrared spectra of pristine UBMOF-31

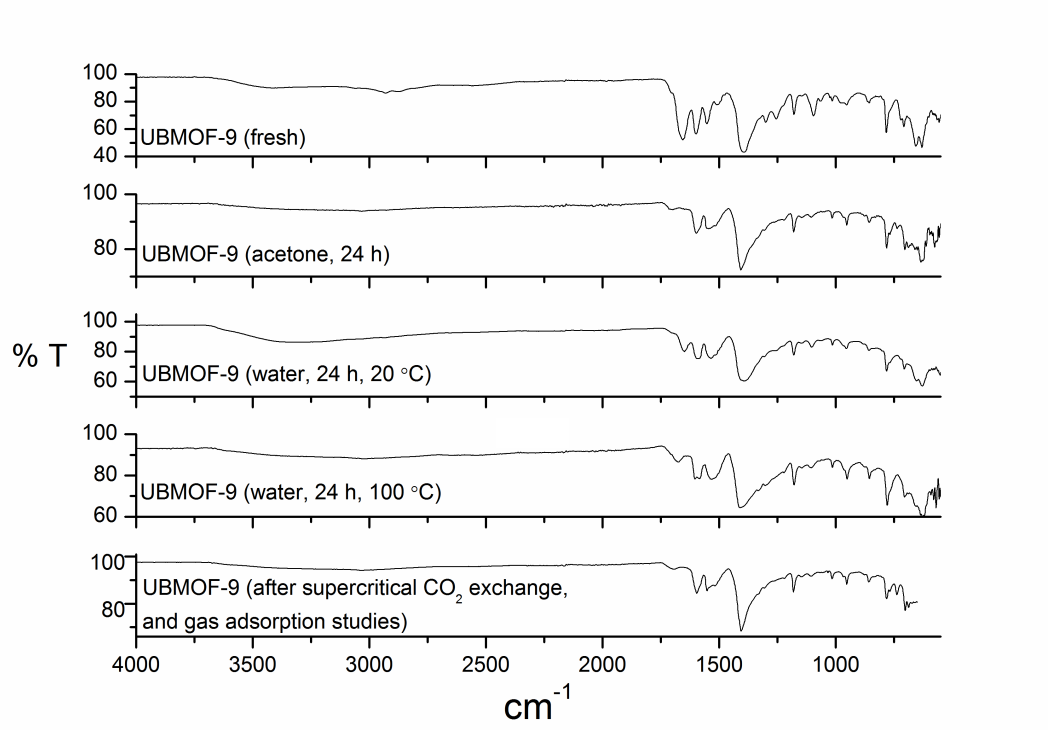


**Figure S4.4.** Comparison of infrared spectra of UBMOF-9 collected for fresh, acetone treated, water treated (20 °C, 24 h), water treated (100 °C, 24 h), and the sample after SC-$CO_2$ treatment and high-pressure gas adsorption studies.

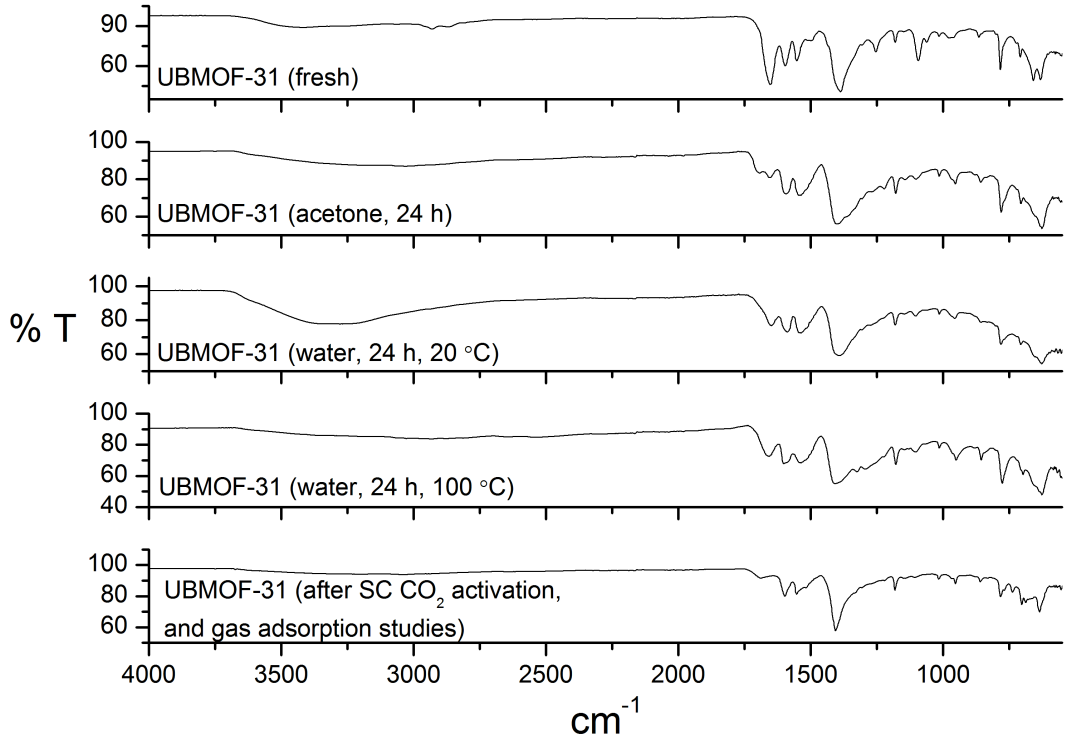


**Figure S4.5.** Comparison of infrared spectra of UBMOF-31 collected for fresh, acetone treated, water treated (20 °C, 24 h), water treated (100 °C, 24 h), and the sample after SC-$CO_2$ treatment and high-pressure gas adsorption studies.

# 5. Sample Images

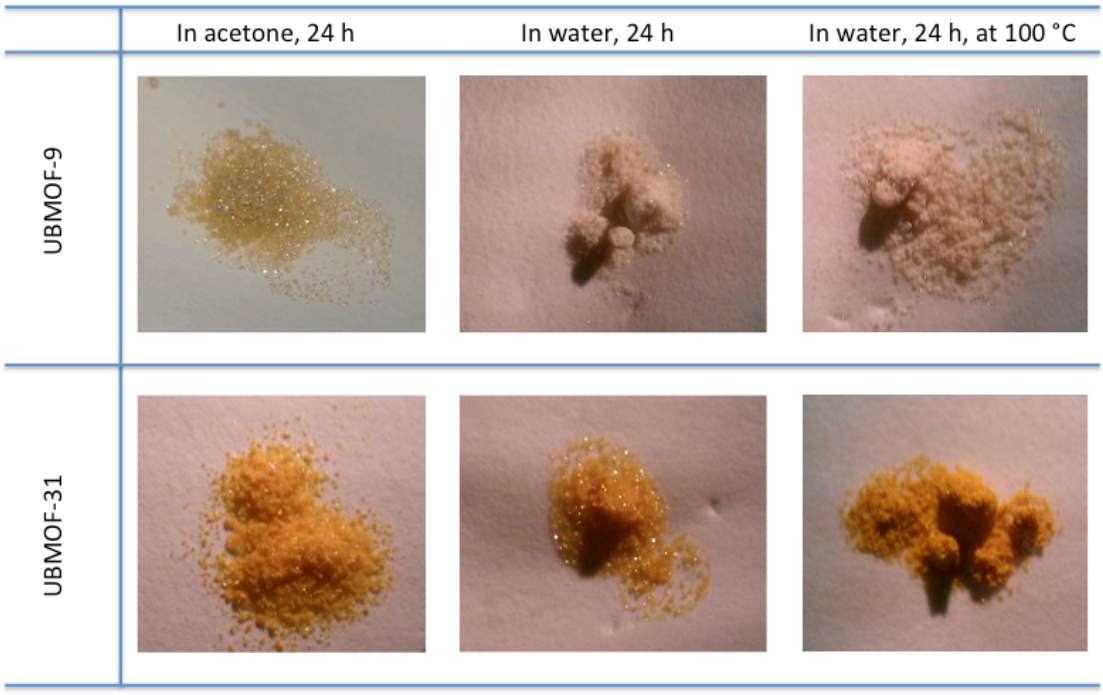


**Figure S5.1.** Optical images of UBMOF-9 and UBMOF-31 treated at different conditions

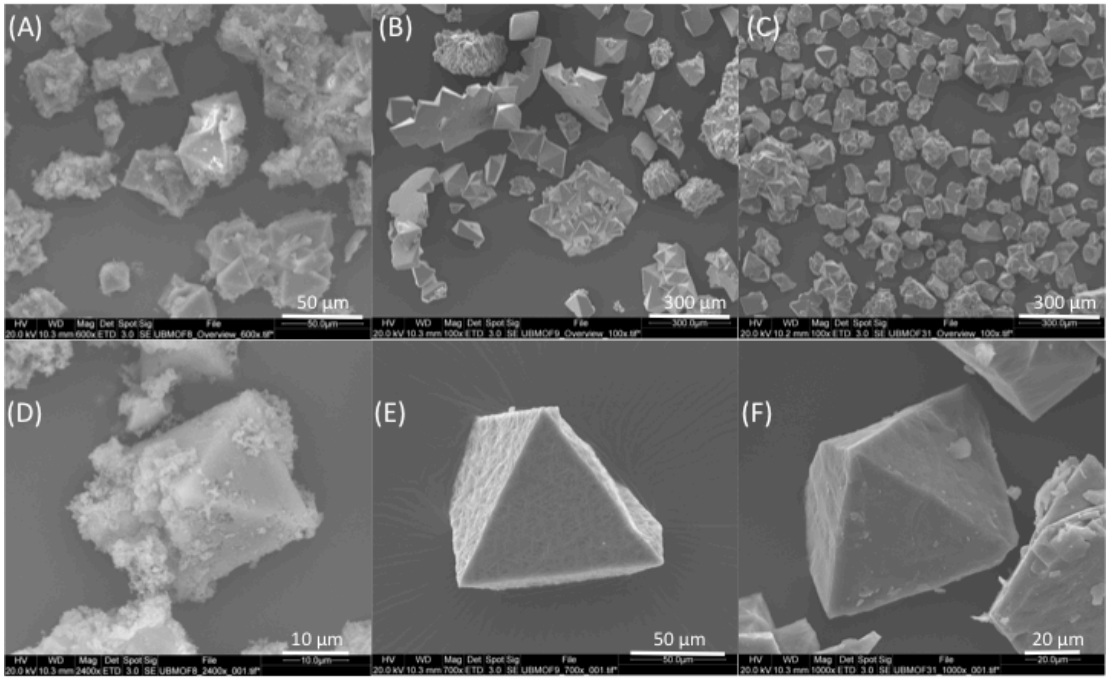


**Figure S5.2.** SEM images of bulk phases of (A) UBMOF-8, (B) UBMOF-9, (C) UBMOF-31 and their close up views D, E, and F, respectively.

# 6. NMR spectra

In three separate vials containing UBMOF-9 (20 mg), UBMOF-31 (20 mg), and UBMOF-31 (20 mg) with added benzoic acid (5 mg), 1 mL of 25 % DCl (in $D_2O$) and 0.5 mL DMSO-$d^6$ was added and sonicated for two hours at 50 °C and left overnight at 25 °C. All samples were then filtered and used for NMR measurements. Measurements with 40 % NaOD were also carried out, but no significant improvements were observed in the peaks originating from the linkers.

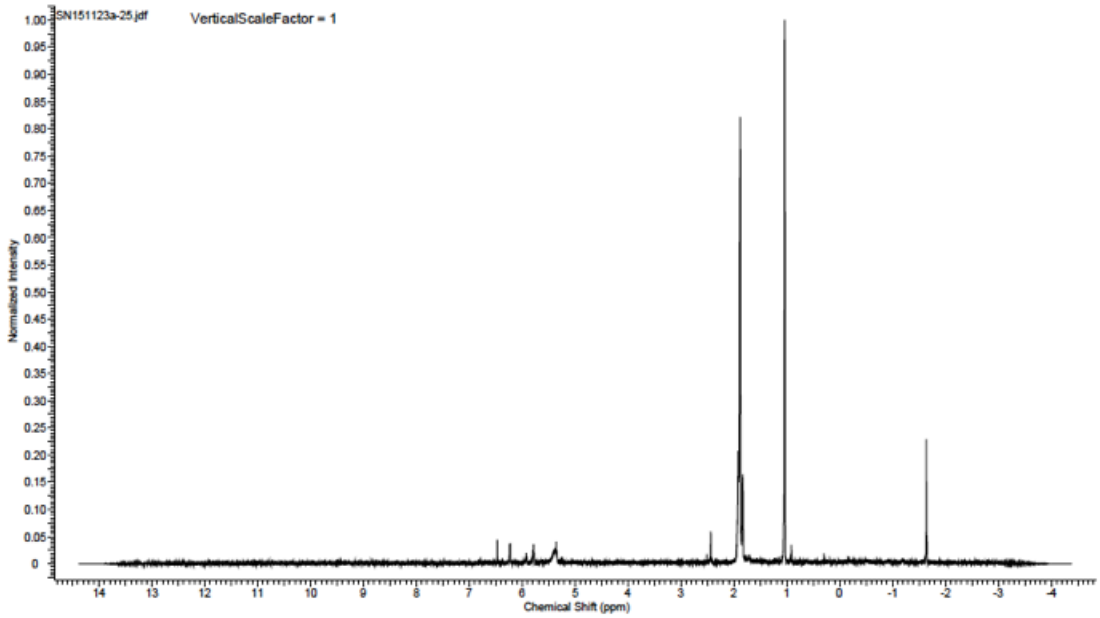


**Figure S6.1.** Full scale NMR spectrum of UBMOF-9

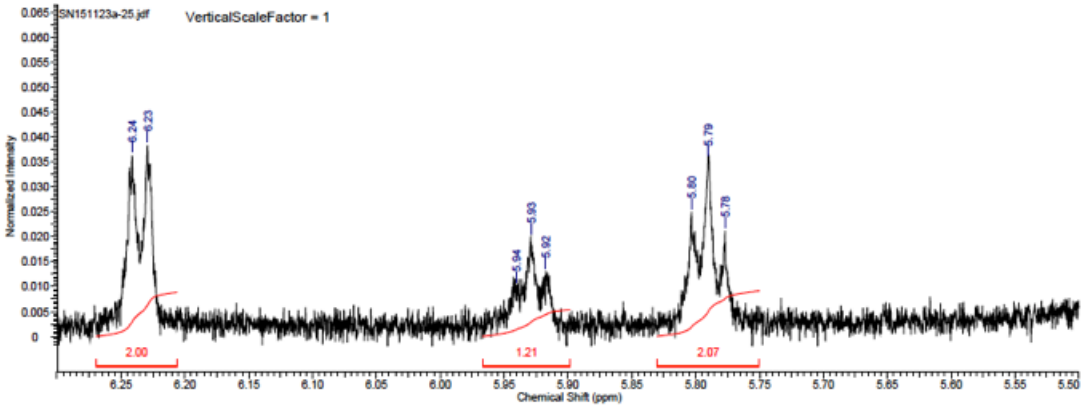


**Figure S6.2.** Selected area of NMR spectrum of UBMOF-9 showing the peaks originating from benzoic acid

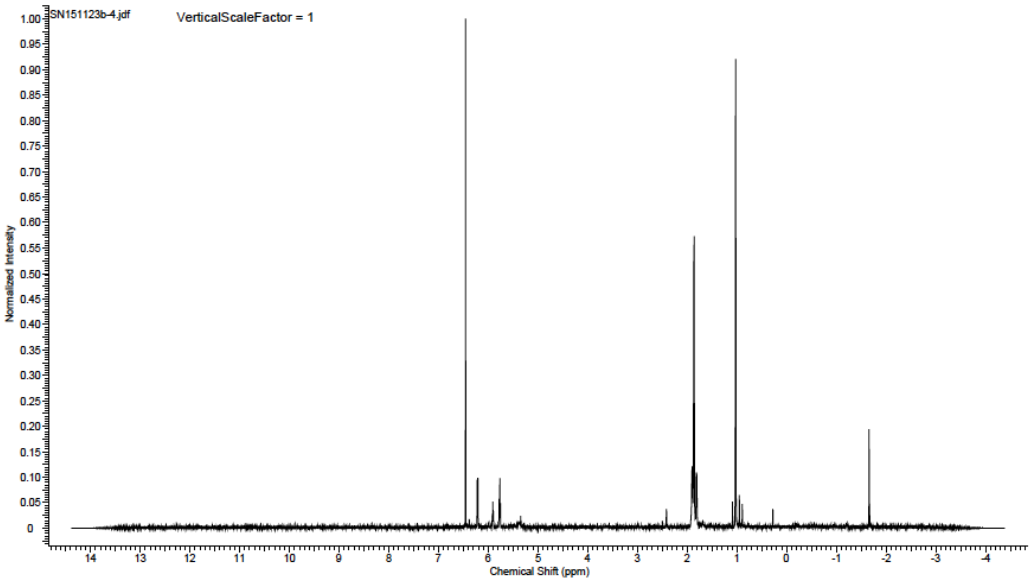


**Figure S6.3.** Full scale NMR spectrum of UBMOF-31

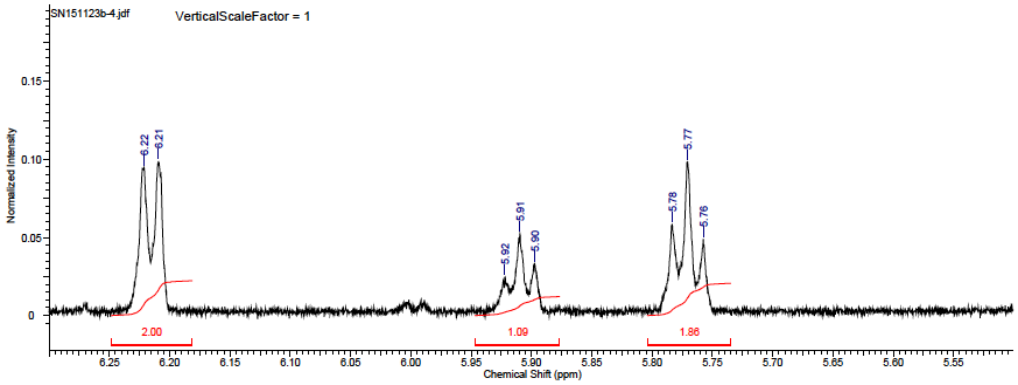


**Figure S6.4.** Selected area of NMR spectrum of UBMOF-31 showing the peaks originating from benzoic acid

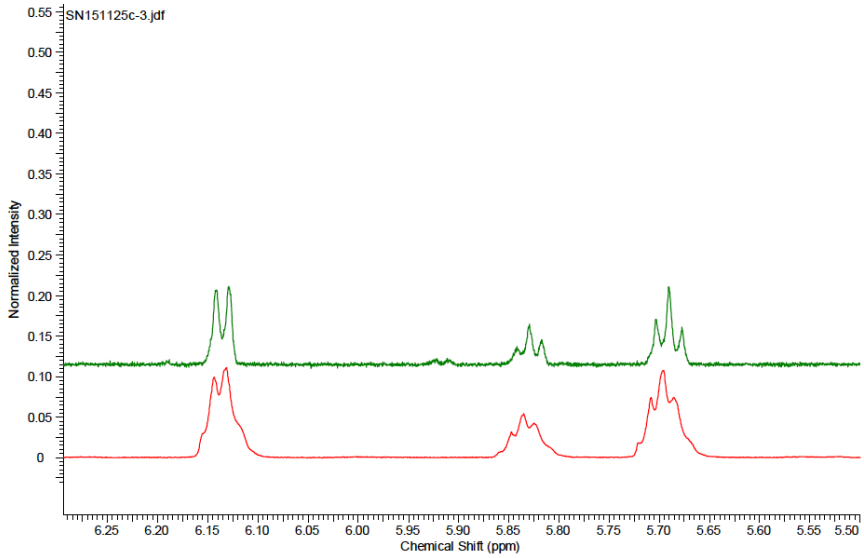


**Figure S6.5.** Comparison of selected area of NMR spectrum of UBMOF-31 (green) and UBMOF-31 with added benzoic acid (red) showing confirming the peaks originating from benzoic acid and poor solubility of the linkers

# 7. Thermogravimetric analyses (TGA)

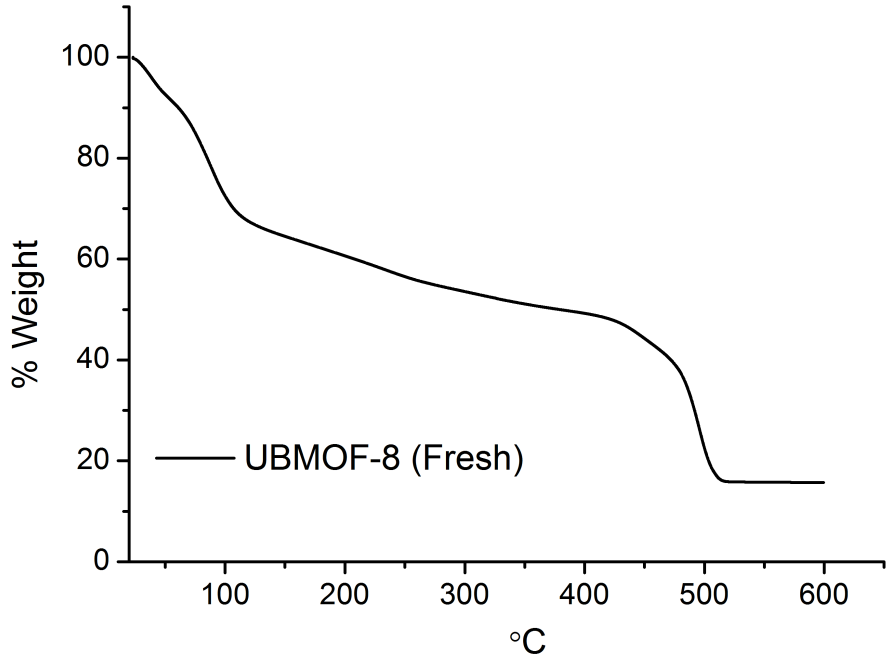


**Figure S7.1.** Thermogravimetric analysis of pristine UBMOF-8 sample

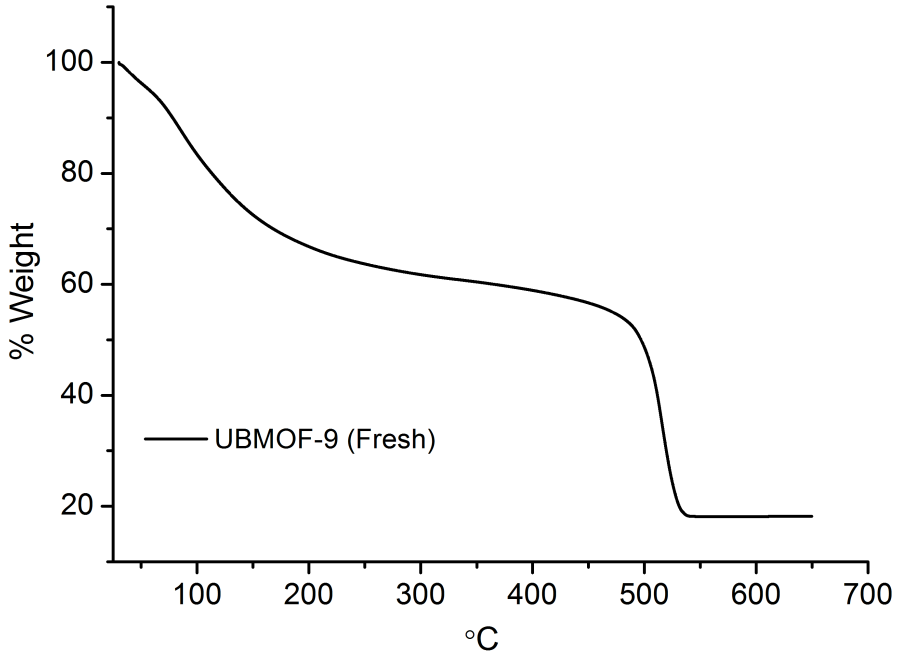


**Figure S7.2.** Thermogravimetric analysis of pristine UBMOF-9 sample

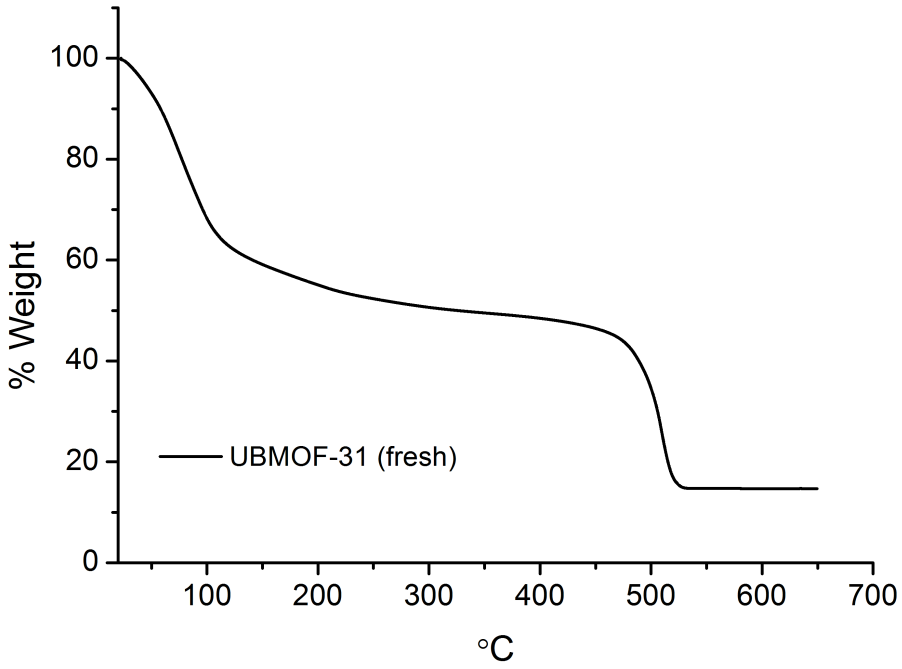


**Figure S7.3.** Thermogravimetric analysis of pristine UBMOF-31 sample

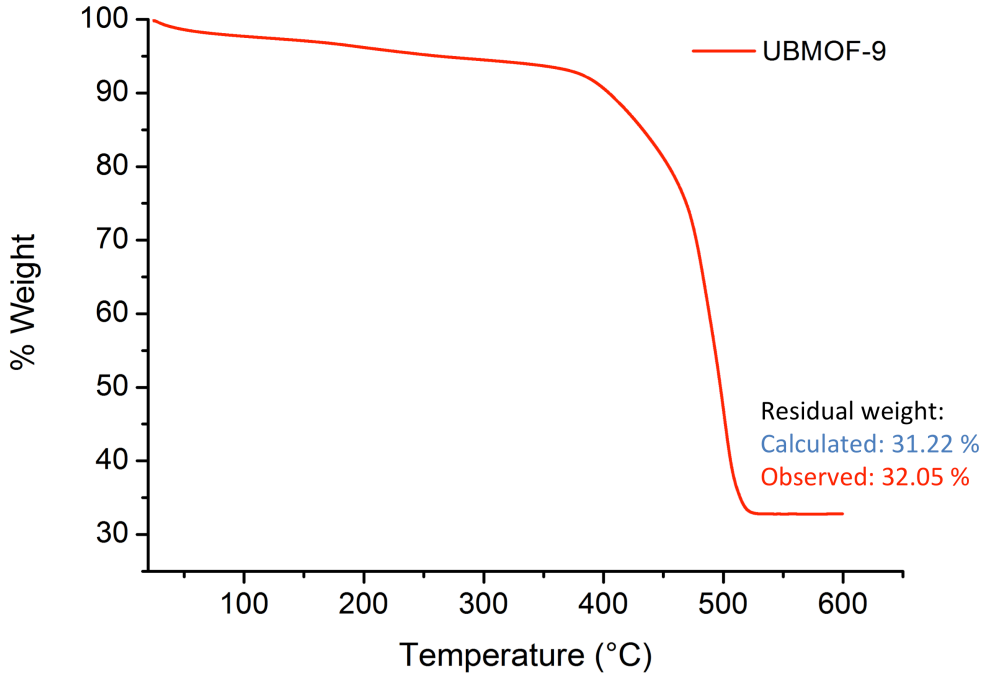


**Figure S7.4.** Thermogravimetric analysis of solvent exchanged dry UBMOF-9 sample (the post-gas adsorption samples were used).

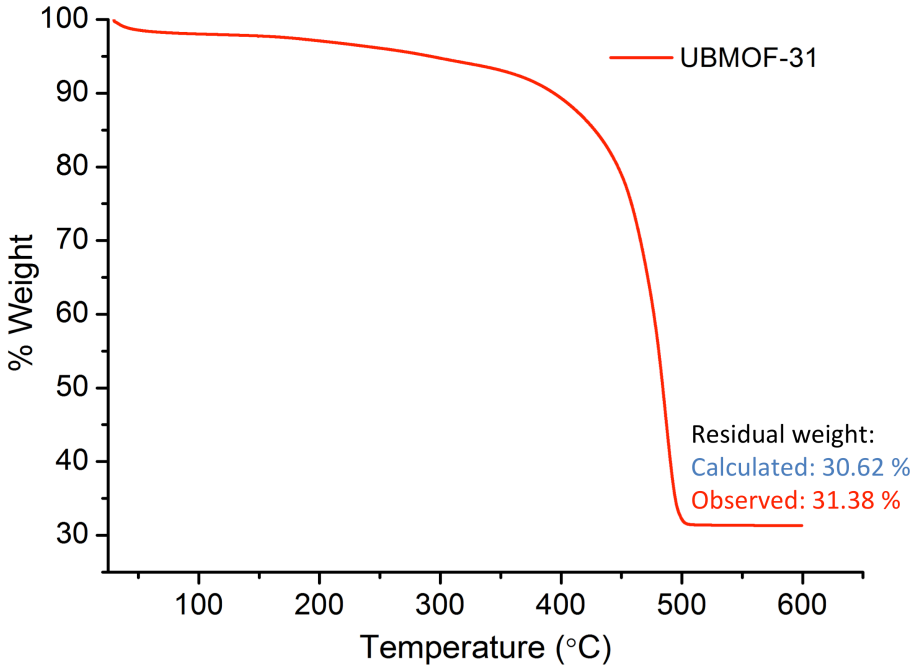


**Figure S7.5.** Thermogravimetric analysis of solvent exchanged dry UBMOF-31 sample (the post-gas adsorption samples were used).

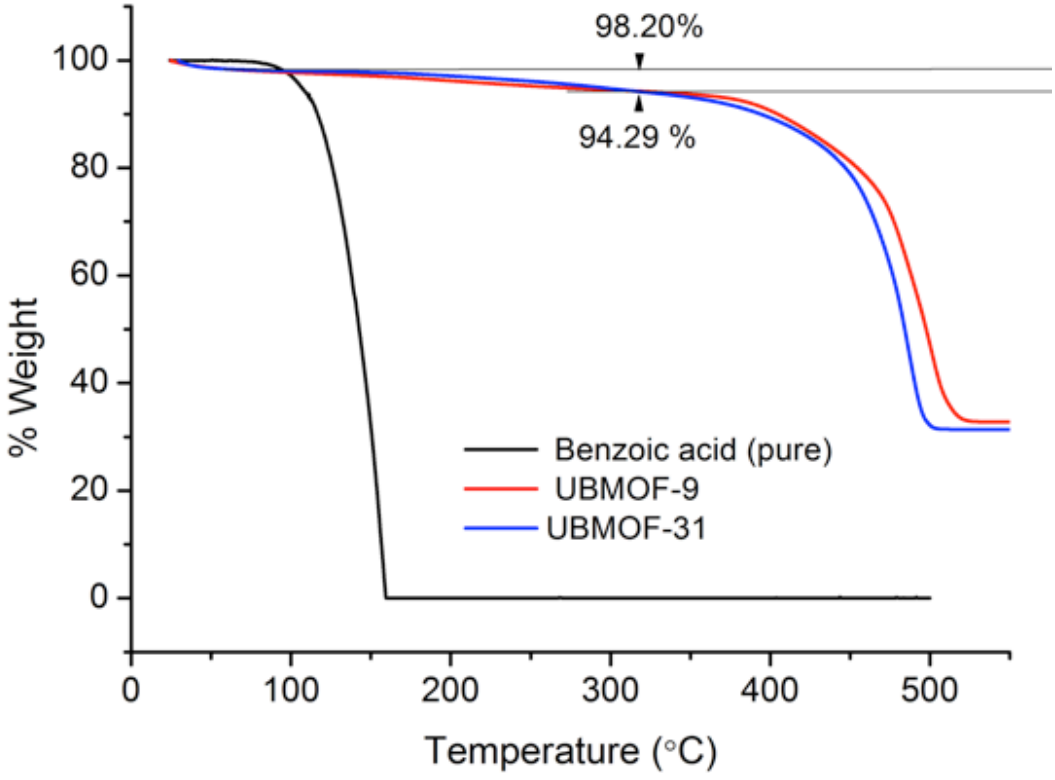


**Figure S7.6.** Thermogravimetric analysis of benzoic acid, and solvent exchanged dryUBMOF-9, and UBMOF-31 to estimate benzoic acid content

# 8. Adsorption studies

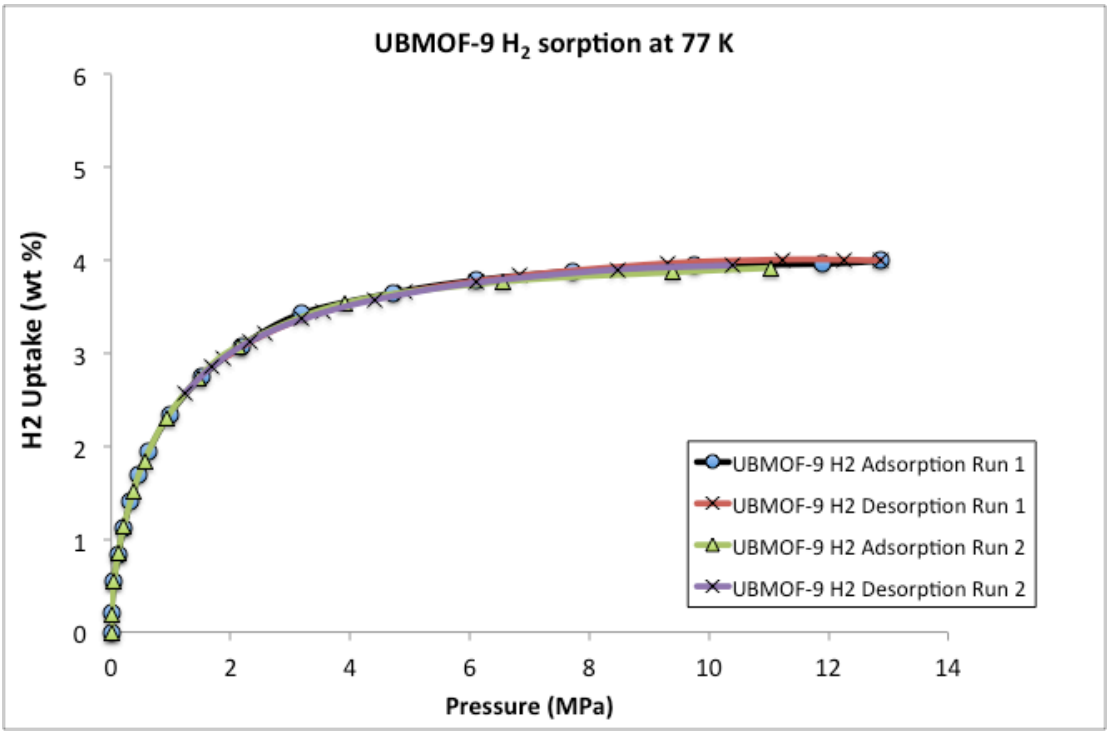


**Figure S8.1.** Repeated hydrogen adsorption-desorption runs at 77 K for UBMOF-9 shows complete reversibility, typical of Type-1 sorption isotherm.

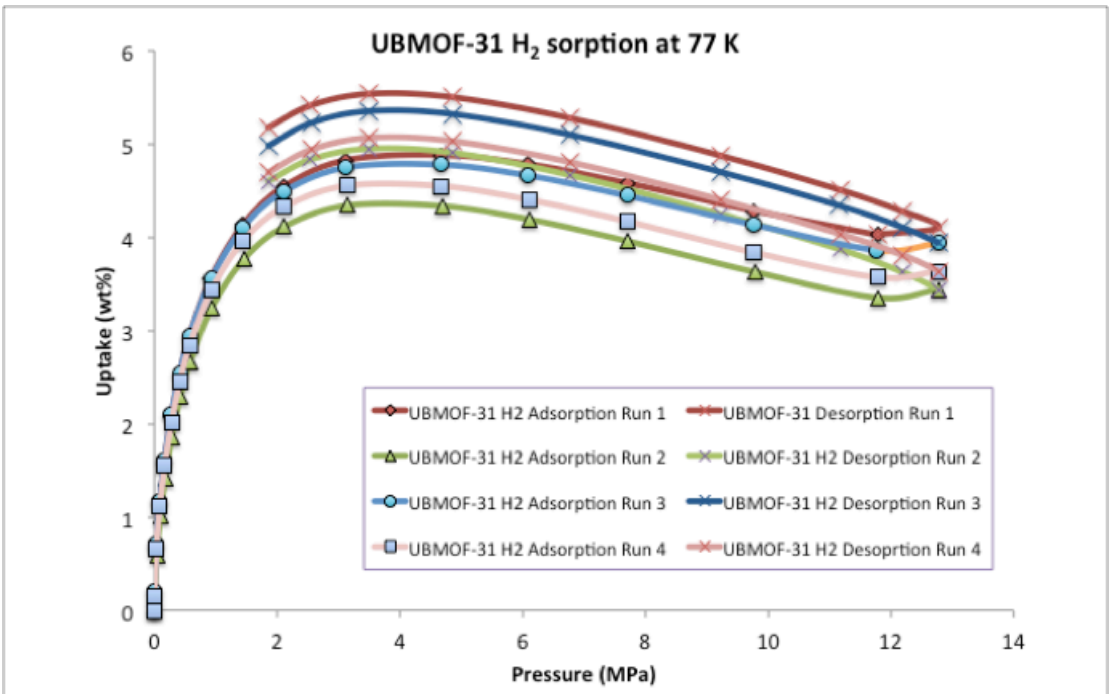


**Figure S8.2.** Hydrogen adsorption-desorption of UBMOF-31 at 77 K shows significant irreversibilites, but higher uptake at low pressures, which could indicate stronger interaction of the framewrok with hydrogen, compared to UBMOF-9.

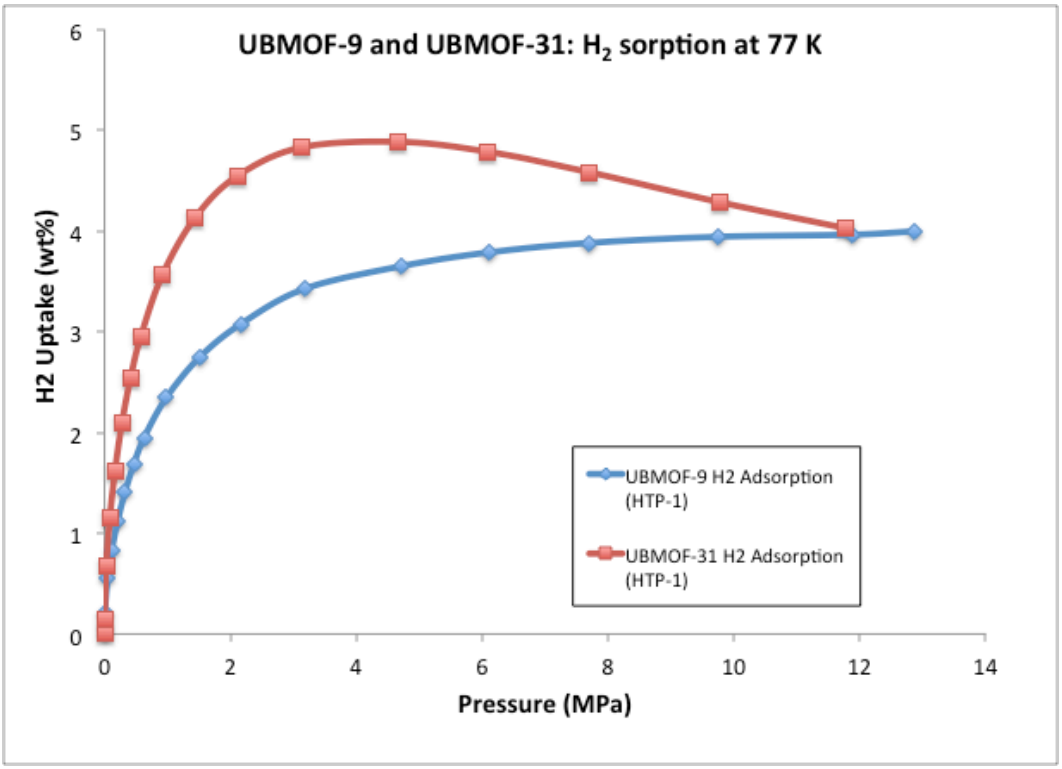


**Figure S8.3.** Comparison of hydrogen uptake between UBMOF-9 and UBMOF-31: UBMOF-31 has higher uptake up to ~12 MPa, but saturates at lower total pressure, possibly due to lower available pore volume in UBMOF-31.

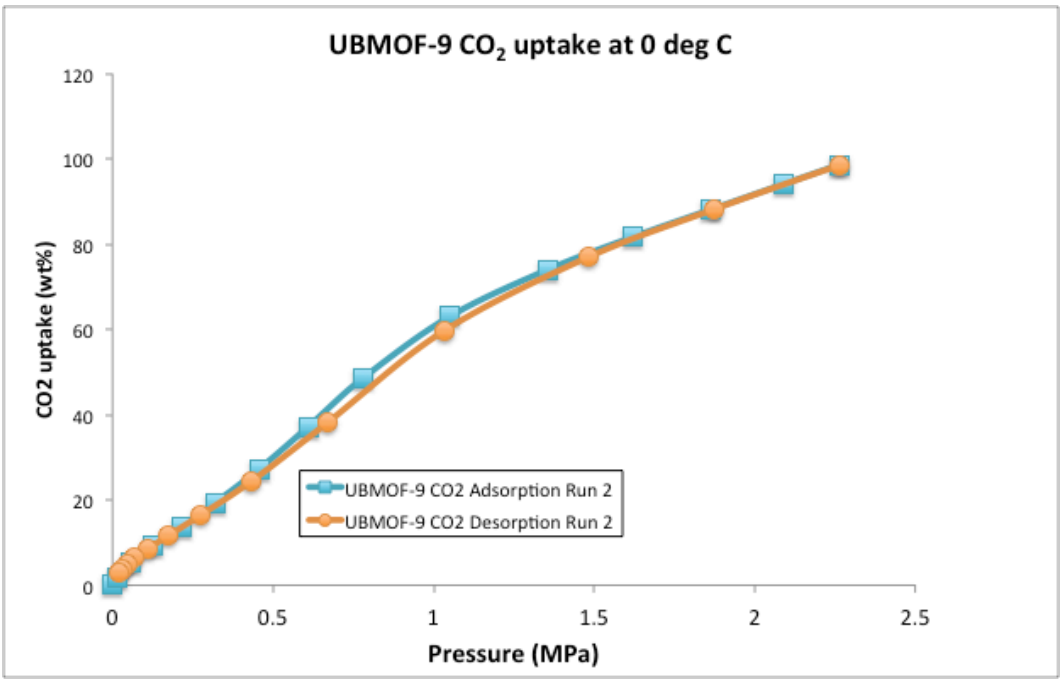


**Figure S8.4.** $CO_2$ sorption at 0 °C for UBMOF-9: Repeated measurements showed good repeatability and reversibility of both $CO_2$ and $N_2$ uptake, indicating pure physisorption.

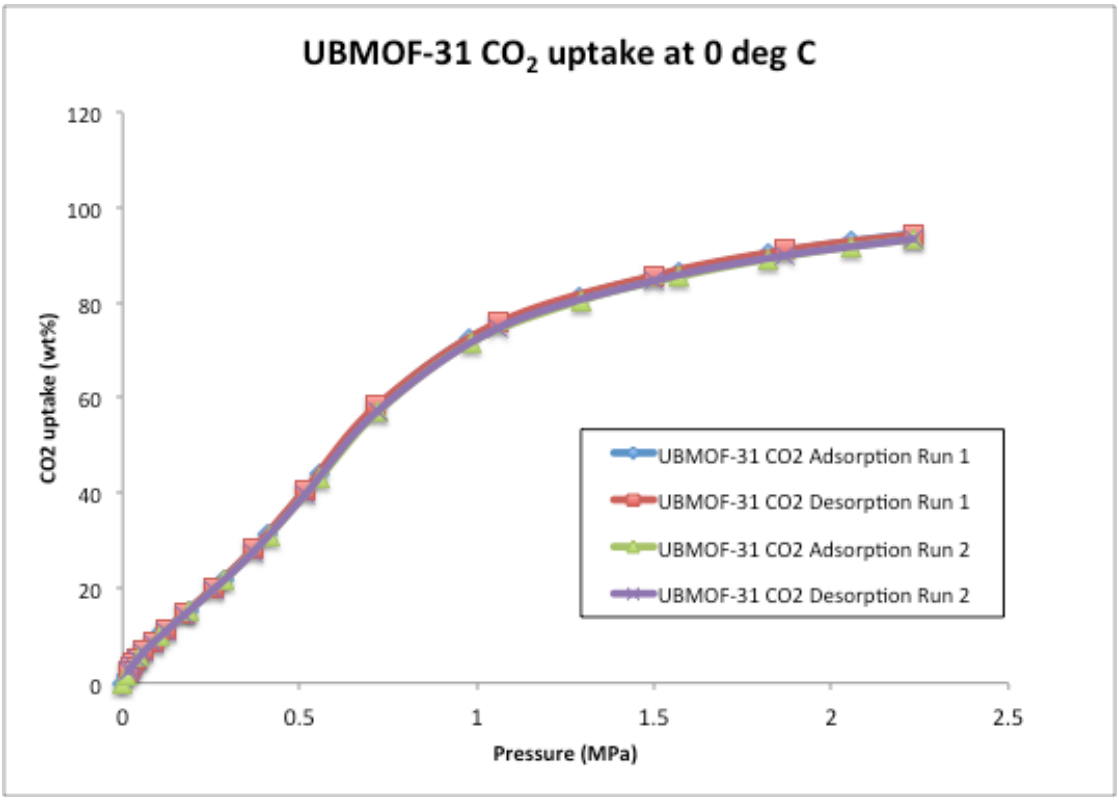


**Figure S8.5.** $CO_2$ sorption at 0 °C for UBMOF-31 (bottom): Repeated measurements showed good repeatability and reversibility of both $CO_2$ and $N_2$ uptake, indicating pure physisorption.

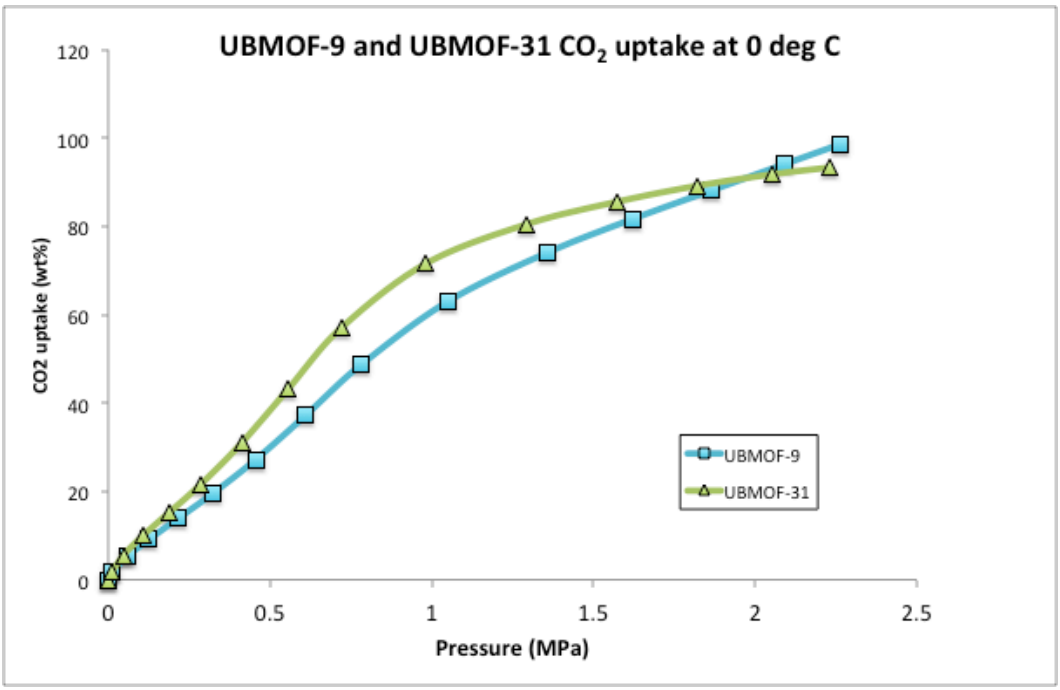


**Figure S8.6.** High pressure $CO_2$ sorption showed comparable total uptake but slight differences in isotherm shapes for UBMOF-9 and UBMOF-31, which may indicate different $CO_2$ sorption sites.

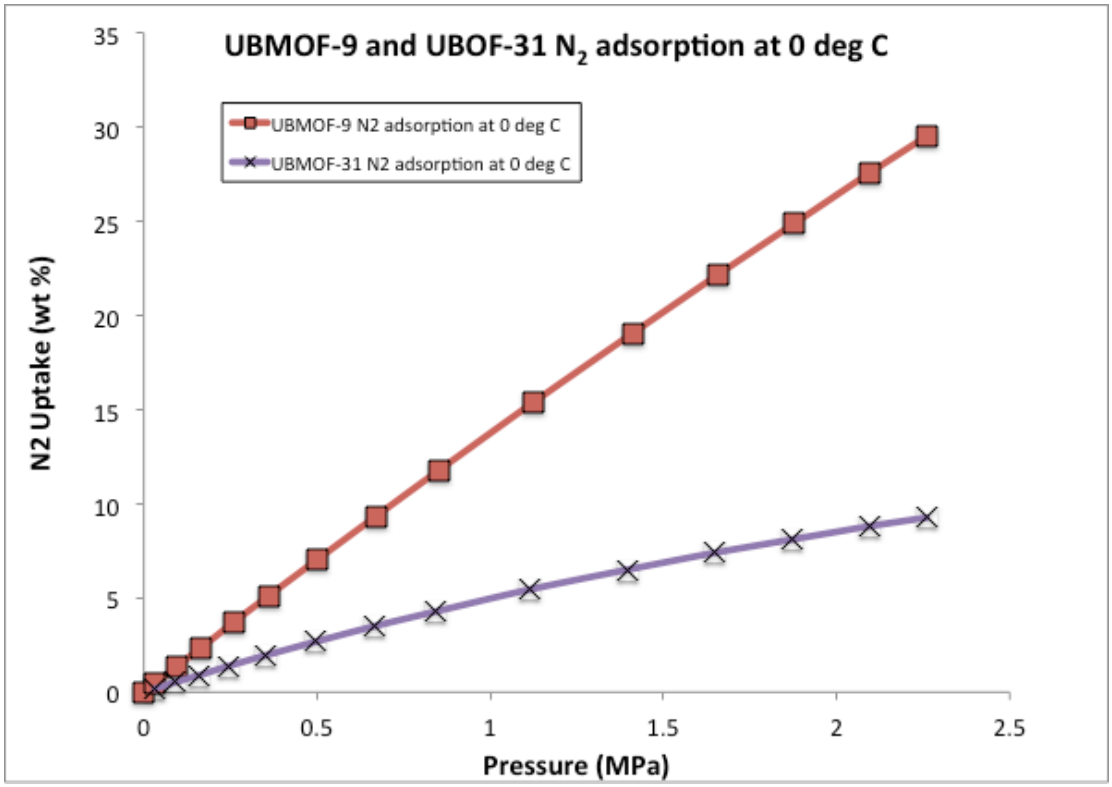


**Figure S8.7.** Comparative $N_2$ sorption at 0 °C over the same pressure range for UBMOF-9 and UBMOF-31.

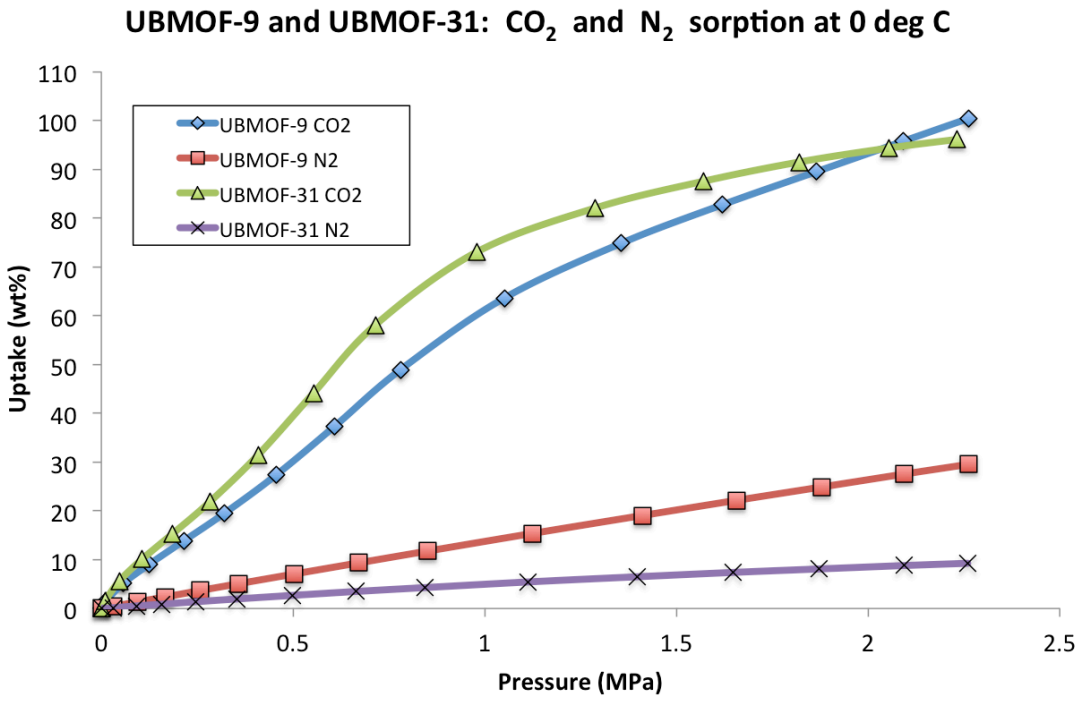


**Figure S8.8.** Comparison between $CO_2$ and $N_2$ uptake: UBMOF-9 and UMBOF-31. UBMOF-9 and UBMOF-31 show similar $CO_2$ uptake behaviour, but UBMOF-31 has a greater affinity for $H_2$ and a greater selectivity ($CO_2$ over $N_2$) than the UBMOF-9

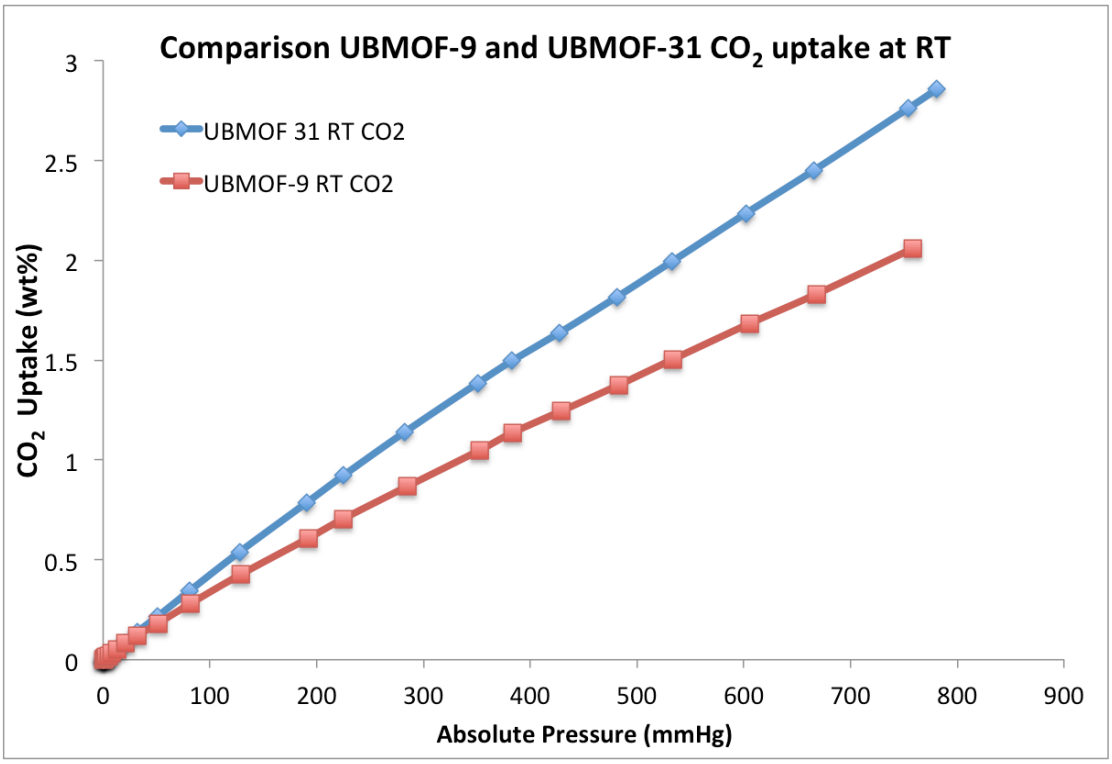


**Figure S8.9.** Comparison of $CO_2$ uptake between UBMOF-9 and UBMOF-31 at room temperature

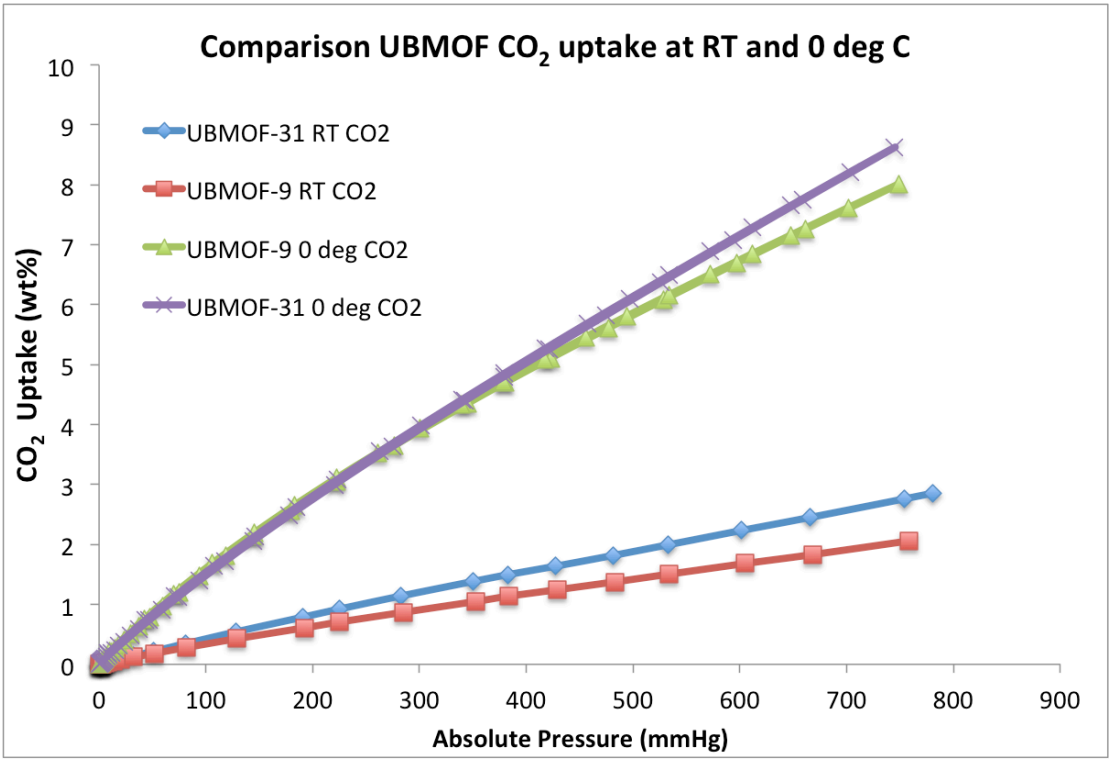


**Figure S8.10.** Comparison of $CO_2$ uptake between UBMOF-9 and UBMOF-31 at room temperature and 273 K

**Determination of volumetric uptake:**

The $H_2$ isotherms of the UBMOF-9 and UBMOF-31 were measured by HTP-1 and modelled using the Tóth equation according to our previously reported methodology [S7, S8], shown in Figure S8.11 and Figure S8.12. The excess isotherm was fit with the Tóth using Equation 1 as the Type I isotherm for calculation of the absolute isotherm (blue line) according to our previous work.

$$m_E = (\rho_A - \rho_B)\theta_A V_p \qquad \text{Equation 1}$$

$$m_A = \rho_A \theta_A V_p = m_E + \rho_B \theta_A V_P \qquad \text{Equation 2}$$

where, $m_E$ and $m_A$ are the excess and the absolute adsorbed amounts in wt.%, respectively. The $\rho_A$ and $\rho_B$ are the adsorbate and bulk density. The $\theta_A$ is the ratio of the adsorbed and $V_P$ is pore volume, which are modelled using Type I Tóth equation [S7]. The absolute isotherm (the blue line) was calculated using Equation 2 and the parameters from the fit, and resulted in an estimated density of the adsorbed $H_2$ of. Hydrogen excess isotherms on UBMOF-9 and UBMOF-31 modeled assuming a constant density of adsorbate resulted in calculated adsorbate densities of 140 ± 18 kg $m^{-3}$ and 73 ± 3 kg/$m^3$, respectively.

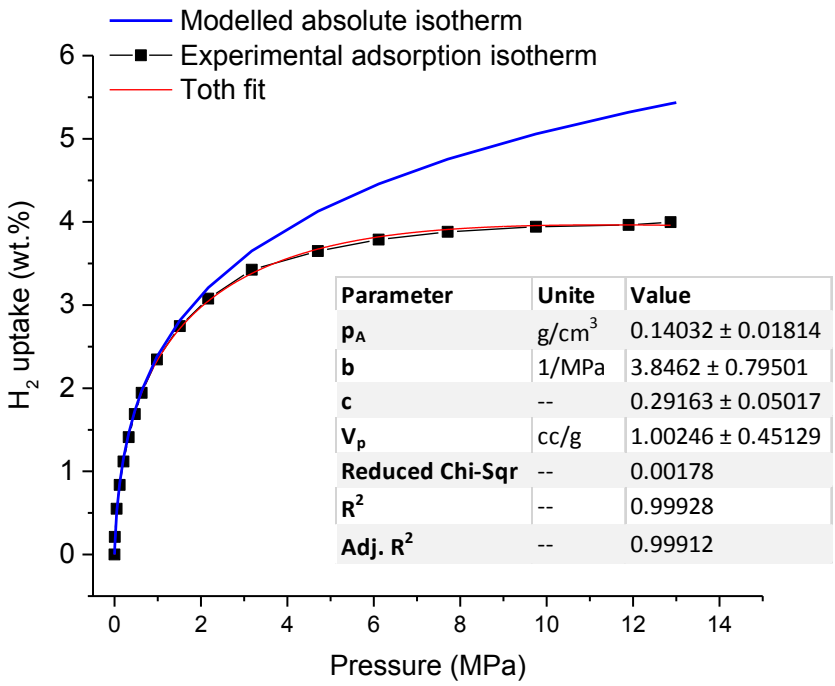


| Parameter | Unite | Value |
|---|---|---|
| $p_A$ | g/cm$^3$ | 0.14032 ± 0.01814 |
| b | 1/MPa | 3.8462 ± 0.79501 |
| c | -- | 0.29163 ± 0.05017 |
| $V_p$ | cc/g | 1.00246 ± 0.45129 |
| Reduced Chi-Sqr | -- | 0.00178 |
| $R^2$ | -- | 0.99928 |
| Adj. $R^2$ | -- | 0.99912 |

**Figure S8.11.** Fitting of excess adsorption isotherm of UBMOF-9 at 77 K with Tóth equation, squares represent the experimental data obtained from HTP-1, the solid red line is the fit to the excess isotherm and the blue line is the absolute isotherm using the Tóth equation. The fit parameters and their standard errors are displayed in the legend.

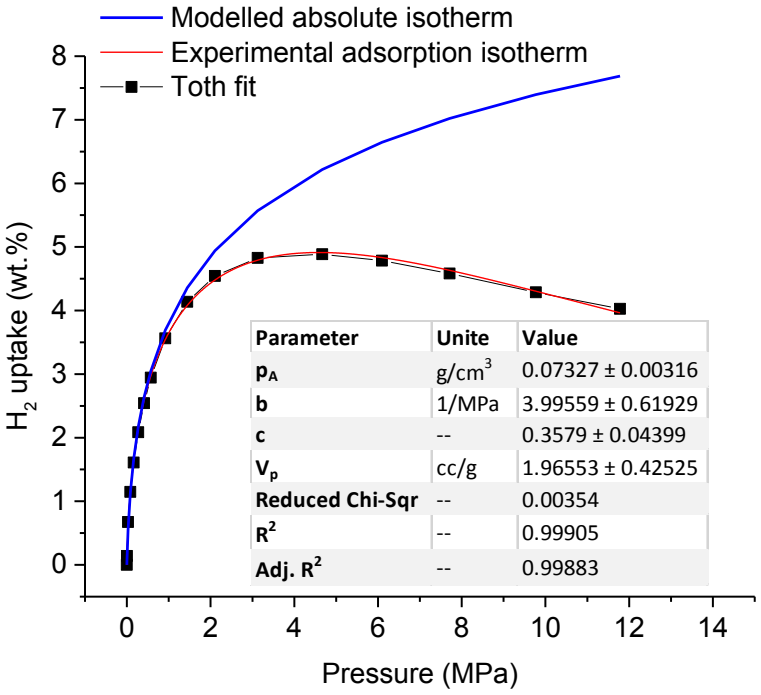


**Figure S8.12.** Fitting of excess adsorption isotherm of UBMOF-31 at 77 K with Tóth equation, squares represent the experimental data obtained from HTP-1, the solid red line is the fit to the excess isotherm and the blue line is the absolute isotherm using the Tóth equation. The fit parameters and their standard errors are displayed in the legend.

**Table S8.1.** Hydrogen uptake by different zirconium based MOFs

| **Material** | **Hydrogen uptake (wt%)** | **Conditions** | **Reference** | **Comments** |
|---|---|---|---|---|
| UiO-66 | 2.4 | 31 bar, 77 K | [S3] | Note the lower % uptake at higher pressure |
| UiO-66 | 2.2 | 80 bar, 77 K | [S3] | |
| UiO-67 | 4.6 | 38 bar, 77 K | [S3] | |
| UiO-67 | 4.2 | 81 bar, 77 K | [S3] | |
| UiO(bpdc) | 5.7 | 20 bar, 77 K | [S4] | |
| Zr-fum MOF | 1.38 | 1 bar, 77 K | [S5] | |
| Cr-MOF@UiO-66 | 2.4 | 1 bar, 77 K | [S6] | |
| UBMOF-9 | 4 | 130 bar, 77 K | This work | |
| UBMOF-31 | 4.9 | 46 bar, 77 K | This work | |

# References:


[S1] G.M. Sheldrick, SHELXTL 5.1, Bruker AXS Inc., 6300 Enterprise Lane, Madison, WI 53719-1173, USA, 1997.
[S2] A. L. Spek, PLATON, A Multipurpose Crystallographic Tool, Utrecht University, Utrecht, The Netherlands 2010.
[S3] S. Chavan, J. G. Vitillo, D. Gianolio, O. Zavorotynska, B. Civalleri, S. Jakobsen, M. H. Nilsen, L. Valenzano, C. Lamberti, K. P. Lillerud and S. Bordiga, *Phys. Chem. Chem. Phys.*, 2012, **14**, 1614-1626.
[S4] L. Li, S. Tang, C. Wang, X. Lv, M. Jiang, H. Wu and X. Zhao, *Chem. Commun.*, 2014, **50**, 2304-2307.
[S5] J. Ren, N. M. Musyoka, H. W. Langmi, B. C. North, M. Mathe, X. Kang and S. Liao, *Int. J. Hydrogen Energ.*, 2015, **40**, 10542-10546.
[S6] J. Ren, N. M. Musyoka, H. W. Langmi, B. C. North, M. Mathe and X. Kang, *Int. J. Hydrogen Energ.*, 2014, **39**, 14912-14917.k
[S7] N. Bimbo, V.P. Ting, A. Hruzewicz-Kolodziejczyk, T.J. Mays, *Farad. Discuss.*, 151 (2011) 59-74.
[S8] N. Bimbo, V.P. Ting, J.E. Sharpe, T.J. Mays, *Colloids Surf., A*, 437 (2013) 113-119.